Phase-sensitive four-wave mixing and Raman suppression in a microstructure fiber with dual laser pumps

J. Fan and A. Migdall

Optical Technology Division, National Institute of Standards and Technology, 100 Bureau Drive, Mail Stop 8441, Gaithersburg, Maryland 20899-8441

Received March 16, 2006; revised June 20, 2006; accepted June 22, 2006; posted June 28, 2006 (Doc. ID 69084); published August 25, 2006

On coupling two phase-coherent frequency-conjugate laser pulses into a microstructure fiber, we observe phase-sensitive photon generation via four-wave mixing, and suppression of Raman emission at the middle frequency. © 2006 Optical Society of America

OCIS codes: 190.4380, 190.5650.

The propagation of light through an optical fiber can be considered as a continuous scattering process with some photons scattering into other frequencies through various nonlinear processes. Some of these nonlinear processes have high gain and lead to many useful applications in optical communication.[1–9] Among fiber optic nonlinearities, four-wave mixing (FWM) is of special interest where two pump photons are annihilated to create a pair of phase-coherent anti-Stokes (ω_{as}) and Stokes (ω_s) photons simultaneously. In the classical realm, this phase coherence is the basis of the phase-sensitive fiber-optic parametric amplifier (FOPA), which provides higher gain and more information carrying capacity than the usual phase-insensitive FOPA.[10–12] In the nonclassical realm, correlated photons are key information carriers.[13–16]

On the other hand, high gain nonlinear processes in an optical fiber can also be detrimental. One example is the Raman process that scatters pump photons individually into Stokes or anti-Stokes wavelengths. In conventional optical communication this causes signal loss and channel-cross talk. In quantum communication Raman scattering produces single photon noise relative to the two-photon information state. In both cases, it would be advantageous to suppress the Raman scattering. One Raman suppression approach makes use of FWM. When FWM phase matching is satisfied, the interaction between the Stokes and anti-Stokes beams can suppress the Raman gain.[17–19] Raman suppression can also be achieved by using dual (or multiple) laser pump beams. With $\omega_{as}-\omega_s=2\Omega_R$ ($\Omega_R=13$ THz is the fiber glass Raman frequency), Raman scattering can be efficiently suppressed at $\omega=\omega_s+\Omega_R$.[20–22] Another approach achieves Raman suppression using fiber birefringence.[23]

In this Letter we study FWM with phase-coherent dual pump pulses.[15] Coupling a pair of phase-coherent frequency-conjugate (with respect to the zero-dispersion wavelength of the fiber) pump pulses into a highly nonlinear microstructure fiber (MF), we show that photon generation at the middle frequency is phase sensitive. When the two pump pulses are in phase, photons are efficiently generated at the middle frequency by FWM. When the two pump pulses are out of phase, the total photon count rates drop below the Raman scattering level, showing a suppression of both FWM and Raman scattering.

The experimental arrangement is shown in Fig. 1. We first generated quasi-super-continuum light by coupling an 8 ps ($\lambda=735$ nm, 80 MHz repetition rate, average power of 16 mW) laser pulse into a MF (MF_1 with a length of 1 m and zero-dispersion wavelength $\lambda_0=735$ nm as specified by the manufacturer), from which we selected a pair of frequency-conjugate pulses (anti-Stokes, 733 nm; and Stokes, 737 nm with 1 nm bandwidths). Using a two-pass grating configuration, the two selected pulses are put back in the same single-spatial mode. The time delay between the two pulses can be adjusted with respect to each

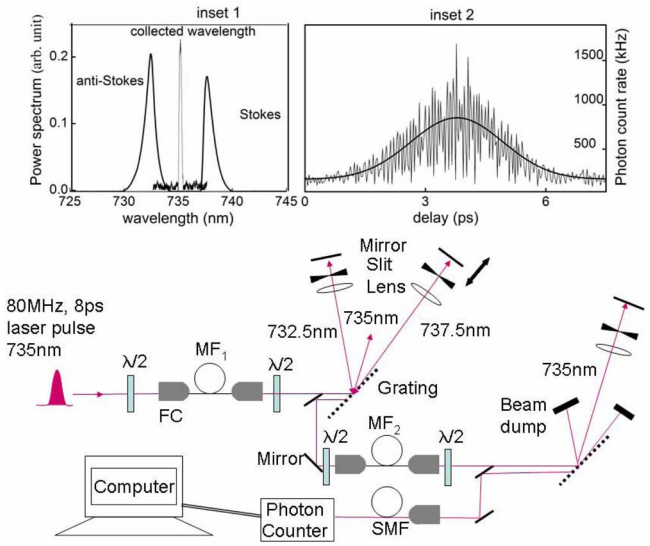

Fig. 1. (Color online) Experimental setup. MF_1 (1 m) and MF_2 (1.7 m), microstructure fibers; FC, fiber coupler; SMF, single-mode fiber; $\lambda/2$, half-wave plate; Ml and M2, mirrors. Inset 1, spectra of the two selected Stokes and anti-Stokes pulses and the collected emission at the exit of MF_2 (pump and FWM spectra were taken at different pump powers). Inset 2, photon count rate at 735 nm with 0.1 nm bandwidth versus delay, fit with a Gaussian function (smooth line).

0146-9592/06/182771-3/$15.00

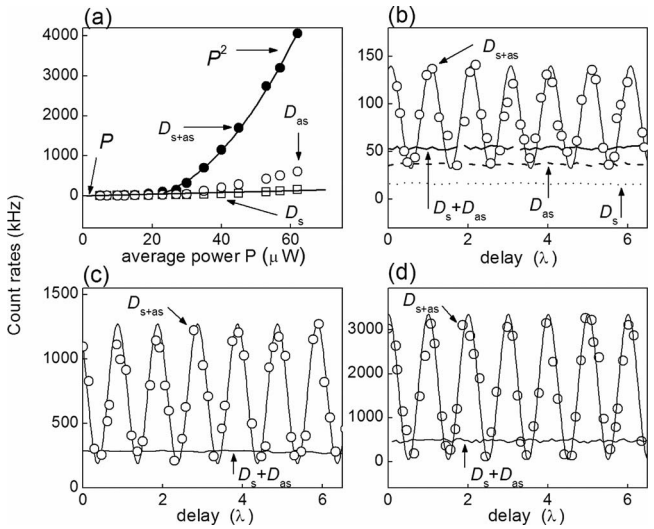

Fig. 2. (a) Detection rates versus average power $P=P_s+P_{as}$ for Stokes–anti-Stokes pump delay optimized for maximum signal. Filled dots, Stokes and anti-Stokes pumps; open dots, anti-Stokes pump only; open squares, Stokes pump only. D_{s+as} is fit with P at lower power and P^2 at higher power. Detection rates versus delay. (b) $P_s+P_{as}=15\ \mu$W, (c) 40 μW, and (d) 55 μW. Dots are experimental data fit to a sine function (smooth curve).

other. The twin pulses are then coupled into a second fiber, MF_2 (identical to MF_1 but 1.7 m long). The light exiting from MF_2 is filtered using a second two-pass grating configuration, selecting $\lambda_0=735$ nm ($\Delta=0.1$ nm) light to be coupled into a single-mode fiber for detection. In the experiment, linear polarization is maintained parallel to the same principal axis of the two MFs, and oriented for maximum grating transmission efficiency.

The spectra of the selected Stokes, anti-Stokes pump pulses, and the collected photons (at $\lambda_0=735$ nm) are shown in Fig. 1 (inset 1). The photon count rate versus the relative delay between the Stokes and anti-Stokes pulses is shown in inset 2. When the Stokes and anti-Stokes pulses are not overlapped in time, the photon count rate at $\lambda_0=735$ nm is a sum of the individual Raman scattering photon rates from the Stokes and anti-Stokes pulses. They are indicated by the level of the wings of the Gaussian curve shown in inset 2. When the two pulses are overlapped in time, the peak photon rate increases by an order of magnitude. This peak results from the nondegenerate FWM process and has been used to prepare two-photon states in our earlier experiments.[15] The photon count rate in inset 2 is strongly modulated. The size and frequency of the modulation suggest that FWM is dependent on the relative phases between the two pulses. This phase sensitivity was examined in detail.

At an optimal delay (with maximum photon count rate), the measured photon count rates D_{s+as}, D_s, and D_{as} for the Stokes+anti-Stokes, Stokes, and anti-Stokes pump configurations, respectively, are shown in Fig. 2(a) versus average pump power P. Note that D_s+D_{as} is the sum of the individual Raman scattering processes (measurement is made when pump pulses do not overlap in time), while D_{s+as} is the photon count rate when the two pulses overlap in time. We see that D_s depends linearly on pump power P, while D_{as} shows a deviation from the linearity, indicating the start of stimulated Raman scattering. At a higher pump power, D_{s+as} shows a clear dependence on P^2, the signature of FWM. This is consistent with our earlier experiments, in which we have shown that two-photon states can be efficiently generated at the middle frequency with $2\omega_0=\omega_s+\omega_{as}$.[15]

The FWM signal was modulated by the relative delay between the two pumps [Figs. 2(b)–2(d)], with a period set by the wavelength. For this FWM process with nondegenerate pumps and degenerate output, under the slowly varying amplitude approximation,[24] the power flow between the Stokes (P_s) anti-Stokes (P_{as}), and the FWM signals (P) can be expressed as

$$\frac{dP_s}{dz}=2\gamma P\sqrt{P_sP_{as}}\sin(\theta), \tag{1a}$$

$$\frac{dP_{as}}{dz}=2\gamma P\sqrt{P_sP_{as}}\sin(\theta), \tag{1b}$$

$$\frac{dP}{dz}=-4\gamma P\sqrt{P_sP_{as}}\sin(\theta), \tag{1c}$$

where the phase difference $\theta=(\beta_s+\beta_{as}-2\beta)z+\delta$, with $\delta=\varphi_{as}+\varphi_s-2\varphi$, where $\beta_{s,as},\beta$, and $\phi_{s,as},\phi$ are propagation wavenumbers and phases for Stokes, anti-Stokes, and FWM photons, respectively. The power flow depends on the phase difference, θ. When $\theta=-\pi/2$, the power flows from two pump beams to generate FWM signals at the middle frequency. When $\theta=\pi/2$, the power flows back to the pumps and the FWM is suppressed. An analysis shows that the nondegenerate FWM gain is a periodic function of $\delta(z=0)$, the phase of the two pump pulses before being coupled into the fiber.[10–12]

In a recent publication on a phase-sensitive parametric amplification process using nondegenerate FWM,[25] passive phase tuning using a fixed-length fiber resulted in a quasi-periodic modulation of the amplification spectrum. In our experiment, the phase difference between the two phase-coherent pump pulses can be actively controlled by varying the optical path length, with periodic modulation of the FWM gain shown with the modulation period set by the wavelength.

Figures 2(b)–2(d) show that FWM signals are well above the Raman scattering level for most delay times, but they drop below the sum of the individual Raman levels, D_s+D_{as} for phase differences of $\theta=\pi/2$, indicating that the Raman process is suppressed along with the suppression of FWM. This suggests that there is an interference between the two Raman scattering processes induced by the Stokes and anti-Stokes pulses.

Classically, using the electric fields of a pair of Stokes and anti-Stokes beams and a degenerate FWM beam, the third-order nonlinear polarization

$P(\omega_0)$ for a harmonic oscillator with resonant frequency ω_r and damping coefficient μ can be derived as[19]

$$P(\omega_0) \propto \left[\frac{2\sqrt{PP_sP_{as}}e^{i\delta}(\omega_r^2-\Delta^2)}{(\omega_r^2-\Delta^2)^2+(2\mu\Delta)^2} + \frac{(P_s+P_{as})\sqrt{P}}{(\omega_r^2-\Delta^2)^2+(2\mu\Delta)^2} + \frac{2i\mu\Delta(P_s-P_{as})\sqrt{P}}{(\omega_r^2-\Delta^2)^2+(2\mu\Delta)^2} \right] e^{i\beta z}, \quad (2)$$

where $\Delta=\omega_{as}-\omega_0=\omega_0-\omega_s$. For simplicity, we assume perfect phase-matching $\beta_s+\beta_{as}-2\beta=0$. The first term accounts for the noninstantaneous nuclear response contribution to FWM with a phase $e^{i\delta}$, which is consistent with the phase-dependent power flow description given above. The second term accounts for the noninstantaneous nuclear response contribution to cross-phase modulation. The third term, which is imaginary, represents stimulated Raman scattering when $P_{as}>P_s$, and inverse Raman absorption when $P_{as}<P_s$. When $P_{as}\approx P_s$, the imaginary term is zero, showing that no photons are generated at ω_0. This is consistent with the recent observations of Raman suppression with dual laser beams,[20–22] in which it was suggested that the Raman susceptibility was canceled via $\mathrm{Im}[\chi_{as}^{(3)R}(\omega_0)+\chi_s^{(3)R}(\omega_0)]\approx 0$. While in that previous experiment, the two pump beams are separated from ω_0 by $\Delta=\omega_{as}-\omega_0=\omega_0-\omega_s=\Omega_R=13$ THz, with pump power greater than the Raman threshold; in our experiment, the two pumps are close to the zero-dispersion wavelength with $\Delta\approx 1$ THz, and the total pump power is much lower than the Raman threshold. Equation (2) also shows that while FWM is sensitive to the phase difference between the Stokes and anti-Stokes beams, the Raman scattering depends only on the relative powers of the two pump beams.

In conclusion, by controlling the relative phase and power of two phase-coherent pump beams, we can simultaneously achieve phase-sensitive FWM amplification, and Raman suppression in an optical fiber. Compared with other similar Raman suppression experiments, the frequencies of our dual pump pulses are close to each other and the pump power is much below the Raman threshold. The result can be qualitatively explained using the third-order classical nonlinear polarization. It is of particular interest as to how much the Raman process can be suppressed relative to the FWM process. In our experiment, the two pump pulses were created from a spontaneous FWM process and were phase conjugate. Overlapping them in time in a second fiber leads to phase-sensitive processes. On the other hand, these two pulses each individually couples to the fiber thermal reservoir containing phonons with random phases. In this sense, the suppression of the Raman process is determined by the temporal overlapping of the two pulses in the fiber.[20–22] Depopulating the phonon density by cooling the fiber may further bring down the Raman noise.[26] Clearly a quantum mechanical approach is needed to fully understand these processes. We have ongoing efforts in that direction along with further experimental efforts. The method applied in our experiment may have potential applications in the development of fiber-based two-photon sources, phase-sensitive fiber parametric amplifiers, and efficient suppression of Raman scattering in optical and quantum communications.

The authors acknowledge helpful discussions with G. P. Agrawal. This work was supported by the MURI Center for Photonic Quantum Information Systems (ARO/DTO program DAAD19-03-1-0199), the DTO entangled source, and the DARPA/QUIST programs. J. Fan's e-mail address is jfan@nist.gov.

References

1. R. Tang, J. Lasri, P. Devgan, J. E. Sharping, and P. Kumar, Electron. Lett. **39**, 195 (2003).
2. J. Harvey, R. Leonhardt, S. Coen, G. Wong, J. Knight, W. Wadsworth, and P. St. J. Russell, Opt. Lett. **28**, 2225 (2003).
3. S. Radic, C. J. McKinstrie, R. M. Jopson, J. C. Centanni, Q. Lin, and G. P. Agrawal, Electron. Lett. **39**, 838 (2003).
4. C. de Matos, J. Taylor, and K. Hansen, Opt. Lett. **29**, 983 (2004).
5. Y. Deng, Q. Lin, F. Lu, G. Agrawal, and W. Knox, Opt. Lett. **30**, 1234 (2005).
6. J. H. Lee, Z. Yusoff, W. Belardi, M. Ibsen, T. M. Monro, and D. J. Richardson, IEEE Photon. Technol. Lett. **15**, 437 (2003).
7. J. Hansryd, IEEE J. Sel. Top. Quantum Electron. **8**, 506 (2002).
8. J. Lee, IEICE Trans. Electron. **E88C**, 327 (2005).
9. S. Radic, IEICE Trans. Electron. **E88C**, 859 (2005).
10. C. J. McKinstrie, Opt. Express **12**, 4973 (2004).
11. M. Vasilyev, Opt. Express **13**, 7563 (2005).
12. C. J. McKinstrie, Opt. Lett. **257**, 146 (2006).
13. X. Li, P. Voss, J. E. Sharping, and P. Kumar, Phys. Rev. Lett. **94**, 053601 (2005).
14. J. G. Rarity, J. Fulconis, J. Duligall, W. J. Wadsworth, and P. St. J. Russell, Opt. Express **13**, 534 (2005).
15. J. Fan, A. Dogariu, and L. J. Wang, Opt. Lett. **30**, 1530 (2005).
16. J. Fan, A. Migdall, and L. J. Wang, Opt. Lett. **30**, 3368 (2005).
17. K. Blow, IEEE J. Quantum Electron. **25**, 2665 (1989).
18. E. Golovchenko, P. V. Mamyshev, A. N. Pilipetskii, and E. M. Dianov, IEEE J. Quantum Electron. **26**, 1815 (1990).
19. R. W. Boyd, *Nonlinear Optics* (Academic, 1992).
20. P. Tchofo Dinda, G. Millot, and S. Wabnitz, J. Opt. Soc. Am. B **15**, 1433 (1998).
21. T. Sylvestre, H. Maillotte, and E. Lantz, Electron. Lett. **34**, 1417 (1998).
22. T. Sylvestre, H. Maillotte, P. Tchofo Dinda, and E. Coquet, Opt. Commun. **159**, 32 (1999).
23. P. Tcholo Dinda, S. Wabnitz, E. Coquet, T. Sylvestre, H. Maillotte, and E. Lantz, J. Opt. Soc. Am. B **16**, 757 (1999).
24. G. P. Agrawal, *Nonlinear Fiber Optics* (Academic, 1995).
25. R. Tang, J. Lasri, P. Devgan, V. Grigoryan, P. Kumar, and M. Vasilyev, Opt. Express **13**, 10483 (2005).
26. L. F. Lee, J. Chen, C. Liang, X. Li, P. L. Voss, and P. Kumar, Opt. Lett. **31**, 1905 (2006).